Title

Cone Spacing Correlates With Retinal Thickness and Microperimetry in Patients With Inherited Retinal Degenerations.

Journal

Investigative ophthalmology & visual science, 60(4)

ISSN

0146-0404

Authors

Foote, Katharina G
De la Huerta, Irina
Gustafson, Kevin
et al.

Publication Date

2019-03-01

DOI

10.1167/iovs.18-25688

Peer reviewed

Cone Spacing Correlates With Retinal Thickness and Microperimetry in Patients With Inherited Retinal Degenerations

Katharina G. Foote,[1,2] Irina De la Huerta,[2] Kevin Gustafson,[2] Angela Baldwin,[2] Shiri Zayit-Soudry,[2] Nicholas Rinella,[2] Travis C. Porco,[2,3] Austin Roorda,[1] and Jacque L. Duncan[2]

[1]School of Optometry and Vision Science Graduate Group, University of California, Berkeley, Berkeley, California, United States
[2]Ophthalmology, University of California, San Francisco, California, United States
[3]Francis I. Proctor Foundation, University of California, San Francisco, California, United States

Correspondence: Jacque L. Duncan, Department of Ophthalmology, University of California, San Francisco, 10 Koret Way, K113, San Francisco, CA 94143-0730, USA; Jacque.duncan@ucsf.edu.

Submitted: September 6, 2018
Accepted: February 13, 2019

Citation: Foote KG, De la Huerta I, Gustafson K, et al. Cone spacing correlates with retinal thickness and microperimetry in patients with inherited retinal degenerations. *Invest Ophthalmol Vis Sci*. 2019;60:1234–1243. https://doi.org/10.1167/iovs.18-25688

Purpose. To determine whether high-resolution retinal imaging measures of macular structure correlate with visual function over 36 months in retinal degeneration (RD) patients and normal subjects.

Methods. Twenty-six eyes of 16 RD patients and 16 eyes of 8 normal subjects were studied at baseline; 15 eyes (14 RD) and 11 eyes (6 normal) were studied 36 months later. Adaptive Optics Scanning Laser Ophthalmoscopy (AOSLO) was used to identify regions of interest (ROIs) with unambiguous cones at baseline to measure cone spacing. AOSLO images were aligned with spectral-domain optical coherence tomography (SD-OCT) and fundus-guided microperimetry results to correlate structure and function at the ROIs. SD-OCT images were segmented to measure inner segment (IS) and outer segment (OS) thickness. Correlations between cone spacing, IS and OS thickness and sensitivity were assessed using Spearman correlation coefficient ρ with bootstrap analyses clustered by person.

Results. Cone spacing ($\rho = 0.57$, $P < 0.001$) and macular sensitivity ($\rho = 0.19$, $P = 0.14$) were significantly correlated with eccentricity in patients. Controlling for eccentricity, cone spacing Z-scores were inversely correlated with IS ($\rho = -0.29$, $P = 0.002$) and OS thickness ($\rho = -0.39$, $P < 0.001$) in RD patients only, and with sensitivity in normal subjects ($\rho = -0.22$, $P < 0.001$) and RD patients ($\rho = -0.38$, $P < 0.001$). After 36 months, cone spacing increased ($P < 0.001$) and macular sensitivity decreased ($P = 0.007$) compared to baseline in RD patients.

Conclusions. Cone spacing increased and macular sensitivity declined significantly in RD patients over 36 months. High resolution images of cone structure correlated with retinal sensitivity, and may be appropriate outcome measures for clinical trials in RD.

Keywords: adaptive optics scanning laser ophthalmoscopy, optical coherence tomography, microperimetry

Retinitis pigmentosa (RP) refers to a diverse group of hereditary retinal degenerative disorders that all cause progressive, diffuse, and relentless loss of photoreceptors, resulting in vision loss and, ultimately, blindness. RP is a leading cause of hereditary blindness in developed countries and affects 1 in 3500 people worldwide.[1] RP manifests with nyctalopia, progressive visual field constriction, and eventual decline in visual acuity. Loss of visual function accompanies fundus findings, including retinal pigment epithelium (RPE) changes, arteriolar attenuation, waxy optic disc pallor, and variable bone spicule pigmentation.[2] RP can occur in isolation or as part of a syndrome that involves other organs, such as Usher syndrome, which is characterized by sensorineural hearing loss in addition to retinal degeneration (RD).[1] Although RP is characterized clinically by degeneration and death (first of rod, followed by cone photoreceptors), RP is genetically heterogeneous and has been associated with mutations in over 60 genes (www.Retnet.org, accessed January 23, 2019), each of which may affect rod and cone survival differently.

Because photoreceptor death is slowly progressive over many years, it has been challenging to demonstrate whether treatments and cures are safe and effective. Specific, reliable, precise, objective, and sensitive measures of photoreceptor health and survival are urgently needed to expedite development of treatments to prevent blindness, monitor disease progression, and measure response to therapies.

Previous studies have shown that measures of visual function in RP correlate with the integrity of the photoreceptor layers imaged using spectral-domain optical coherence tomography (SD-OCT).[3–5] However, current SD-OCT techniques lack sufficient resolution for examination of individual photoreceptors, raising the possibility that subtle changes in photoreceptor structure are being missed. In contrast, adaptive optics scanning laser ophthalmoscopy (AOSLO) has been used to visualize the retina with lateral resolution at the single cell level,[6,7] enabling imaging of the cone mosaic and measurement of cone spacing and density, and AOSLO has been used to study eyes with inherited retinal degenerations.[8–10] Cone density and

spacing correlate with clinical measures of visual function including visual acuity and foveal sensitivity in RD,[11,12] suggesting that the high-resolution measures of cone structure obtained with AOSLO may be useful in tracking disease progression.[13,14]

However, in eyes with RD, cone spacing and density are not always found to correlate with cross-sectional measures of photoreceptor layer thickness obtained with SD-OCT,[15–17] possibly because rods contribute to measures of outer nuclear layer thickness outside the fovea, and some cones have diminished reflectivity,[18–20] accounting for decreased cone density measures in regions with normal cross-sectional thickness. Confocal AOSLO images of photoreceptors are generated by light reflected at the photoreceptor inner segment/outer segment (IS/OS) and OS/RPE junctions,[21] while the cell bodies of degenerating photoreceptors may persist in the outer nuclear layer (ONL) even after the IS and OS have degenerated.[22] Thus, it is possible that areas with intact photoreceptor cell bodies that have degenerating IS and OS with reduced visual function could show no correlation between cone spacing or density and cross-sectional measures of ONL thickness from OCT scans. Prior studies have demonstrated a correlation between cone spacing measures with AOSLO and visual function at the fovea in patients with retinal degenerations,[12] and parafoveal cone density has been correlated with spatial contrast sensitivity[23] and multifocal electroretinography,[24] but the relationship between retinal structure and visual sensitivity, when measured using microperimetry to assess function at macular locations outside the central fovea, has not been previously reported on a cellular level in RP.

The current study was designed to test the hypothesis that cone spacing measures from confocal AOSLO images correlate with typical clinical structural and functional measures, including spectral domain OCT and fundus-guided microperimetry. High-resolution measures of macular structure and function were analyzed in eyes imaged at baseline and again 36 months later in patients with RD and age-similar, visually normal subjects. Structural measures of outer retinal health—including cone spacing from en face high-resolution images acquired with AOSLO and thickness of the IS and OS layers on SD-OCT scans—were compared with functional measures of visual sensitivity from fundus-guided microperimetry at identical retinal locations in normal eyes and in eyes with RD. The results may help improve current measures of detection and progression of RD to monitor the outcome of therapeutic interventions over 36 months.

Methods

Study Design

This study was approved by the Institutional Review Boards of the University of California, San Francisco and the University of California, Berkeley, and adhered to the tenets of the Declaration of Helsinki. All subjects provided written informed consent.

Clinical Examination

Best-corrected visual acuity (BCVA) and refractive error were measured according to the Early Treatment of Diabetic Retinopathy (ETDRS) study protocol.[25] Axial length was measured using partial coherence interferometry (IOL Master; Carl Zeiss Meditec, Dublin, CA, USA). Genetic testing was performed in 2 patients (40032 and 30007, respectively) as previously described.[26,27] Twelve patients (30015, 40023, 40030, 40043, 40046, 40039, 40064, 40067, 40070, 40079, 40080, and 40082) were tested using next-generation sequencing of 181 genes in a retinal dystrophy panel that included copy number analysis (Blueprint Genetics, San Francisco, CA, USA) through the genetic testing study of the Foundation Fighting Blindness My Retina Tracker registry for inherited retinal degenerative diseases (NCT 0245940).

SD-OCT Data Collection and Cross-sectional Thickness Measurements

Spectral-domain optical coherence tomography (SD-OCT, Spectralis HRA+OCT system; Heidelberg Engineering, Vista, CA, USA) images analyzed included 20° or 30° horizontal and vertical cross section B-scans through the fovea. SD-OCT images were segmented manually to measure inner and outer segment (IS and OS) length at locations corresponding to regions of interest (ROIs) using custom software to measure inner and outer segment thickness at locations 0.1 degree apart.[5,28–32] Examples of segmented horizontal OCT B-scans for an RD patient (40039) are shown in Supplementary Figure S1.

Microperimetry Analysis

Fundus-guided microperimetry was obtained as formerly described[28] (Nidek MP1, NAVIS software, ver. 1.7; Nidek Technologies, Fremont, CA, USA) under light-adapted conditions (32 cd/m^2) with spot size V (104 arcmin diameter, 1.73 degrees) delivered for 200 milliseconds under a 4-2-1 threshold strategy. With this staircase algorithm, threshold estimates are measured so that if the subject responds affirmatively that they are able to see the stimulus, the subsequent stimulus appears 4 dB dimmer until a reversal occurs (once the patient responds negatively that they cannot see the stimulus), and then the stimulus appears 2 dB brighter until a second reversal occurs. Following the second reversal, the stimulus is adjusted by 1 dB until the third reversal, at which point the threshold estimate is produced. A 3-degree diameter red ring was used as a fixation target, and patients were instructed to look in the center of the red ring after correcting for refractive error and presbyopia to focus the stimuli on the retina for each patient (Microperimeter MP1 Operator's Manual; Nidek Technologies Srl 2003–2016, p 23). Fundus-guided perimetric sensitivity was determined at locations spaced 2 degrees apart along the horizontal and vertical meridians through the fovea in the central 10 degrees surrounding fixation. To ensure the light-adapted measurement isolated cone function, sensitivity was determined with a long-pass dichroic filter (605 nm; NT30-634; Edmund Optics, Barrington, NJ, USA).

AOSLO Image Acquisition and Cone Spacing Analysis

High-resolution images were acquired with Adaptive Optics Scanning Laser Ophthalmoscopy (AOSLO) and processed as described previously.[8,12,13] Regions of interest (ROIs) were selected at locations within 5.7 degrees of the fovea at which unambiguous cones were visualized in AOSLO images acquired at baseline to improve the likelihood that the cones could be monitored longitudinally. For each subject AOSLO images were aligned with the near-infrared (NIR) SLO fundus images acquired with the SD-OCT and the microperimeter (Adobe Illustrator; Adobe, Inc., San Jose, CA, USA) to permit direct comparisons between measures of retinal structure and function (Fig. 1). Eight to 12 ROIs that aligned with the horizontal and vertical SD-OCT scans acquired through the fovea were selected from each AOSLO montage. Chosen for

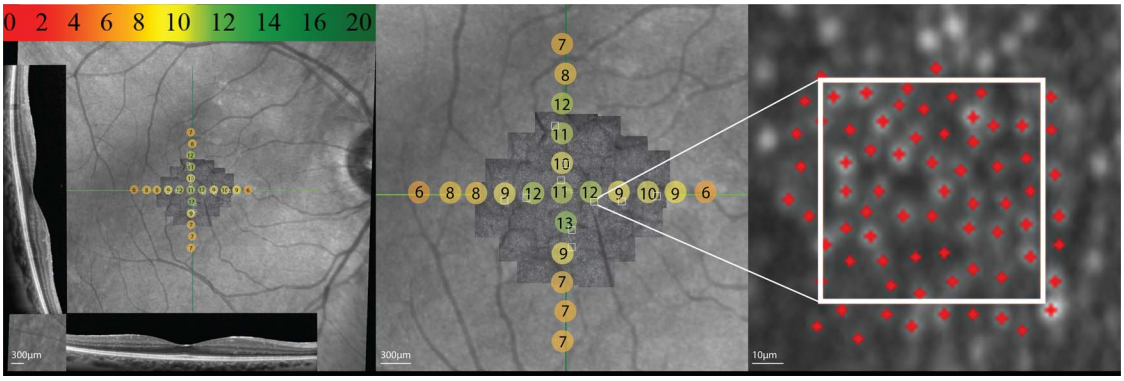

Figure 1. Adaptive optics scanning laser ophthalmoscopy (AOSLO) image, spectral domain-optical coherence tomography (SD-OCT) horizontal and vertical scans, and fundus-guided microperimetry map superimposed in patient 30015 OD. (**A**) Macular sensitivity values in color-coded circles are shaded from *green* (normal) to *red* (stimulus not seen) based on the sensitivity measured at each location; color scale bar at *top* of panel; *scale bar*: 300 µm. (**B**) Magnified view of (**A**); regions of interest (ROIs) are outlined in *white boxes*; small white pixels indicate the patient's preferred retinal locus of fixation; *scale bar*: 300 µm. (**C**) Magnified view of ROI N1. *Red crosses* indicate positions of cones used to assess cone spacing; *scale bar*: 10 µm.

analysis in the present study was a subset of ROIs that corresponded to regions tested using MP1 stimuli and located within 1 degree of the center of a given MP1 location. The average distance from the center of the ROI to the center of the region stimulated with the MP1 stimulus was 0.37 degrees (standard deviation 0.29, range: 0–1 degree), so most of the ROIs were well within the size of the MP1 stimulus. Cone spacing (or average nearest neighbor distance) was measured by 1 to 5 graders using a density recovery profile method[33] with custom-written software, as previously described.[8,17] The distance from the foveal center to the center of each ROI was measured in degrees. Cone spacing was measured in arcminutes and converted into Z-scores representing the number of standard deviations from the mean of 27 normal subjects[11] to control for eccentricity. For subjects imaged more than once, precise alignment of follow up images with baseline images ensured the same locations were measured and images were analyzed in random order.

Comparisons for Statistical Analysis

For each patient, macular sensitivity and average IS and OS thickness at each ROI were compared to cone spacing Z-scores, controlling for visit year, using a Spearman correlation with bootstrap clustered by person to establish that data from both eyes of some subjects were included. In addition, IS thickness and OS thickness were compared to sensitivity.

Results

Study Subjects

Twenty-six eyes of 16 patients with RD and 16 eyes from 8 normal control subjects were studied at baseline (Table 1). Of those, 15 eyes of 14 patients with RD and 11 eyes from 6 visually normal control subjects were studied longitudinally 36 months later (Table 2). Patient 40023 developed cystoid macular edema at 36 months which precluded reliable cone spacing measures at ROIs that were visible at baseline. RD patients 10048, 30007, 30015, 40030, 40032, 40043, 40046, 40064, 40067, 40070, 40079, 40080, and 40082 participated in a clinical trial of an experimental treatment for RP, administered to only one eye randomly selected for each subject; after the baseline visit treated eyes were excluded from analysis at 36 months and only the sham-treated eye was analyzed at the 36-month visit (labeled "study eye" in Table 1). One RD patient (40026) and 2 normal controls (10017 and 40048) left the study after completing the baseline visit but before completing the 36-month visit. The control subjects were age-similar (mean ± standard deviation = 46 ± 11.2 years) to, but slightly older than, the patients (mean ± standard deviation = 38 ± 10.5 years, *t*-test $P = 0.07$). The mean BCVA was better in the normal group (20/16) than in the patient group (20/20) (*t*-test $P < 0.0001$).

Due to a variety of causes—including patient drop out, relocation, or participation in a clinical treatment trial—not all eyes of all subjects studied with SD-OCT, AOSLO, and MP1 at baseline were imaged using the same measures 36 months later. Similarly, not all subjects participated in the MP1 experiments or, due to unstable fixation, the MP1 data was found unreliable at both baseline and 36-month visits. The numbers of values for each of the analyzed measures are listed in Table 2.

Figure 2 presents eccentricity and cone spacing for all patients and normal subjects. Cone spacing measures and eccentricity were significantly correlated for patients ($\rho = 0.57$, 95% confidence interval (CI): 0.37 to 0.79, $P < 0.001$) and normal subjects ($\rho = 0.90$, 95% CI: 0.87 to 0.92, $P < 0.001$). The average eccentricity of measurements was lower in patients (1.46 degrees) compared to normal subjects (1.87 degrees) (*t*-test $P < 0.0001$; Fig. 2). This is expected because retinal degeneration precluded measurement at greater eccentricities in some patients where cone loss extended within the region imaged using AOSLO.

Structural and Functional Correlations

Structural and functional correlations described here are summarized in Table 3. Cone spacing was significantly and negatively correlated with IS and OS thickness in patients and normal subjects (Figs. 3A, 3B; Table 3). However, when cone spacing Z-scores were used to control for eccentricity, cone spacing Z-scores were not significantly correlated with IS or OS thickness in normal eyes but were both significantly and negatively correlated with IS and OS thickness in RD patients (Figs. 3C, 3D; Table 3).

Functional Correlations

Photoreceptor IS thickness and OS thickness were not significantly correlated with macular sensitivity in patients,

Investigative Ophthalmology & Visual Science

Table 1. Summary of Clinical Information for Patients and Normal Control Subjects in this Study

AOSLO ID	Sex	Age (y)	Diagnosis/Mutation	Eye	Baseline Acuity	36-Month Acuity	Refractive Error
10048	F	40	Multiplex RP/Unknown	OD	20/25	20/32*	−1.25+1.25x080
				OS	20/20		−1.25+1.25x120
30007	F	27	Usher syndrome type 3: homozygous *CLRN1* mutations c.144T>G, p.Asn48Lys (pathogenic)	OD	20/20	20/20*	−1.50+0.75x170
				OS	20/20		−0.75+0.50x030
30015	M	40	Simplex RP/*PRPH2* c.634A>G, p.Ser212Gly (likely pathogenic)	OD	20/20	20/20*	−2.75DS
				OS	20/20		−2.50DS
40023	M	34	Simplex RP/NGS: *PDE6B:* c.1624C>T, p.Arg542Trp and c.2140A>T, p.Met714Leu (both variants of uncertain significance)	OD	20/25	N/A	+0.50+1.25x118
				OS	20/25		plano+1.25x075
40026	F	28	Simplex RP/no genetic testing	OD	20/25	N/A	−1.25+0.25x075
				OS	20/20		−1.25+0.50x100
40030	F	40	Simplex RP/negative NGS	OD	20/16	20/13*	−3.75DS
				OS	20/16		−3.75DS
40032	M	30	ARRP: compound heterozygous *RPE65* mutations (c.1451G>A, p.Gly484Asp and c.746A>G, p.Tyr249Cys) and homozygous *ABCA4* mutations (c.5882G>A, p.Gly1961Glu)	OD	20/25	20/25*	−3.75+4.00x092
				OS	20/20		5.00+4.25x080
40043	F	30	ARRP: compound heterozygous mutations in *USH2A* (c.2276G>T, p.Cys759Phe and deletion exons 12-16, c.(1971+1_1972-1)_(3316+1_3317-1)del) (pathogenic)	OD	20/20	20/20*	−1.75+1.00x090
				OS	20/20		−2.25+1.00x075
40046	M	62	Simplex RP/negative NGS	OD	20/20	20/20*	plano+0.50x082
				OS	20/25		plano+0.75x100
40039	M	45	ARRP: *USH2A*: c.2276G>T, p.Cys759Phe and c.2296T>C, p.Cys766Arg (pathogenic)	OD	20/20	20/20	−8.75+2.50x137
				OS	20/16	20/16	−7.25+1.25x040
40064	M	18	XLRP: *RPGR* hemizygous c.1243_1244delAG, p.Arg415Glyfs*27 (pathogenic)	Study eye	20/25	20/25	−8.75+2.50x137
40067	M	42	Simplex RP, negative NGS	Study eye	20/20	20/16	−0.50+0.00x000
40070	F	39	Simplex RP, *IFT140* c.634G>A, p.Gly212Arg (pathogenic) and c.1390G>T, p.Val464Leu (likely pathogenic); one inherited from each parent	Study eye	20/16	20/20	−1.50+0.50x090
40079	M	53	ADRP: *PRPF31* c.1273 C>T, p.Gln425* (likely pathogenic)	Study eye	20/16	20/20	−0.75+1.00x010
40080	M	30	XLRP: *RPGR* hemizygous c.28+5 G>A (likely pathogenic)	Study eye	20/20	20/16	−4.25+0.50x090
40082	M	40	ARRP: *USH2A* c. 8522G>A, p.W2841 and c.11266 G>A, p.G3756S, (likely pathogenic); one inherited from each parent	Study eye	20/25	20/25	−4.75+0.25x090
10017	F	31	Normal	OD	20/16	N/A	−0.25DS
				OS	20/16		−0.50DS
10023	M	57	Normal	OD	20/10	20/16	−1.00+1.00x025
				OS	20/13	N/A	−1.50+1.25x135
10033	M	57	Normal	OD	20/16	20/13	+0.25+0.50x135
				OS	20/16	20/13	+0.50+0.00x000
40048	M	51	Normal	OD	20/13	N/A	−0.50+0.50x075
				OS	20/16		−0.50+0.50x140
40053	F	37	Normal	OD	20/20	20/16	−0.75+0.25x168
				OS	20/13	20/16	−0.25+0.25x015
40054	F	24	Normal	OD	20/16	20/16	−0.25+0.00x000
				OS	20/16	20/16	−0.25+0.25x105
40055	M	50	Normal	OD	20/13	20/13	−0.25+0.00x000
				OS	20/16	20/13	−0.75+0.00x000
40061	M	50	Normal	OD	20/16	20/16	−1.50−1.75x015

* Asterisk indicates study eye used (eye not specified to keep readers masked to the treated eye). M, male; F, female; AR, autosomal recessive; XL, X-linked; OD, right eye; OS, left eye; NGS, next generation sequencing genetic testing; N/A, not available.

Investigative Ophthalmology & Visual Science

Table 2. Summary of Clinical Measures Acquired on Patients and Normal Subjects Used In The Current Study

	OCT & AOSLO		MP1	
Subjects	**BL**	**36mo**	**BL**	**36mo**
Patients				
# patients	16	14	9	9
# eyes	26	15	13	10
Normals				
# subjects	8	6	4	4
# eyes	16	11	8	8

BL, baseline visit; 36mo, 36 months; MP1, fundus-guided microperimetry.

but both were significantly correlated in normal subjects (Figs. 4A–B; Table 4). The correlation was positive, where reduced sensitivity correlated with decreased IS and OS thickness. Patients showed a trend in which reduced IS and OS thickness and sensitivity were observed; the small sample size and variability in sensitivity at regions with normal IS and OS thickness may have reduced the power to detect a significant correlation in patients. However, cone spacing Z-scores were significantly and negatively correlated with macular sensitivity in both normal subjects and patients (Fig. 4C; Table 5), such that increased cone spacing Z-scores correlated with reduced sensitivity for both normal subjects and patients. When cone spacing was greater than 2 standard deviations above the normal mean (Z-scores $\pm$ 2), sensitivity was reduced (Fig. 4C).

Change from Baseline to 36 Months

Comparing measures at baseline to 36 months, cone spacing increased significantly in patients by 0.10 arcminutes (95% CI: 0.059 to 0.14, $P < 0.001$), and cone spacing Z-scores increased significantly in patients by 0.94 (95% CI: 0.52 to 1.31, $P < 0.001$), but cone spacing did not change significantly in normal subjects. In addition, although there was no significant change in normal subjects, mean macular sensitivity decreased by −3.74 dB over 36 months (95% CI: −5.56 to −0.81, $P = 0.007$), indicating loss of macular function in RD patients. There was no significant change between baseline and 36 months in IS thickness or OS thickness in either patients or normal subjects. Baseline measures compared to measures at 36 months are summarized in Table 6.

Discussion

This study presents further evidence that structural cone measures using AOSLO images correlate with cross-sectional thickness measures of the IS and OS layers on SD-OCT.[34–36] Both the IS and OS thickness were correlated with cone spacing measures in the present study of normal eyes and patients with RD; patients in the present study all had rod-cone dystrophy (RP or Usher syndrome type 3), so the results are most relevant for RP patients. However, the correlation of IS, OS, and cone spacing with eccentricity from the fovea did likely influence the observed correlation between cone spacing and OCT measures because IS and OS thickness was significantly correlated with cone spacing Z-score in patients but in not normal subjects, when eccentricity was accounted for using Z-scores. The negative correlation between cone spacing Z-scores and both IS and OS thickness indicates that cone spacing Z-scores increase while outer retinal layer thickness decreases. The difference in correlation strength between OS thickness and cone spacing Z-scores versus IS thickness and cone spacing Z-scores may be related to the sequence in which cone photoreceptors degenerate in patients with RP: OS are the earliest affected, then IS are lost, and the nuclei of cone photoreceptors in the outer nuclear layer are last to degenerate.[22,37] The variation in OS thickness in patients observed in Figures 3B and 3D likely reflects inclusion of patients at different stages of degeneration, with some retaining longer photoreceptor OS while having normal cone spacing Z-scores, but many with shorter OS showing abnormal cone spacing normal Z-scores.

The correlation between IS and OS thickness and sensitivity was significant only in normal subjects. We anticipated that OS thickness would correlate with sensitivity since the OS contain the photoreceptor disc structures that are responsible for phototransduction. However, sensitivity in RD patients was variable, likely due (at least in part) to inclusion of a genetically heterogeneous population. Some of the mutations associated with RP in the present study (such as *PRPH2*) are associated with long OS,[38] while others (such as *PDE6B*) affect phototransduction,[39] or the retinoid cycle (such as RPE65[40]) each of which may affect sensitivity of photoreceptors differently with different OS thickness. Analysis of macular function using fundus-guided microperimetry in a genetically homogeneous patient population may provide clearer insight into the relationship between structure and function in the macula of RD patients. Other research using experimental conditions similar to the present study has reported large variabilities in macular sensitivity for both patients and normal subjects.[28] Lack of significant correlations between sensitivity and IS or OS thickness in RD patients is likely due to the insensitivity of fundus-guided perimetric stimuli when detecting subtle visual loss, due to the variability observed in microperimetric responses and coarse resolution of fundus-guided microperimetric visual function tests.

Another fundus-guided microperimetry study tested macular function in patients with X-linked RP. Using a slightly different protocol—white stimuli, which might have allowed for a mixed rod-cone response—variability was seen as well.[41]

Table 3. Summary of Statistical Analyses from This Study. OCT Thickness Correlated With Cone Spacing

OCT Layer Thickness (μm)	Spearman's Correlation ρ Cone Spacing (arcmin)	95% CI	*P* Value	Fig.	Spearman's Correlation ρ Cone Spacing (Z-scores)	95% CI	*P* Value	Fig.
IS thickness								
Normal subjects	−0.45	−0.56 to −0.32	<0.001	3A	−0.17	−0.31 to 0.011	0.068	3C
Patients	−0.50	−0.65 to −0.40	<0.001		−0.29	−0.61 to −0.090	0.002	
OS thickness								
Normal subjects	−0.52	−0.67 to −0.36	<0.001	3B	−0.1	−0.30 to 0.12	0.36	3D
Patients	−0.59	−0.75 to −0.46	<0.001		−0.39	−0.81 to −0.19	<0.001	

Sig, statistical significance; IS, inner segment; OS, outer segment; μm, microns; dB, decibels.

Investigative Ophthalmology & Visual Science

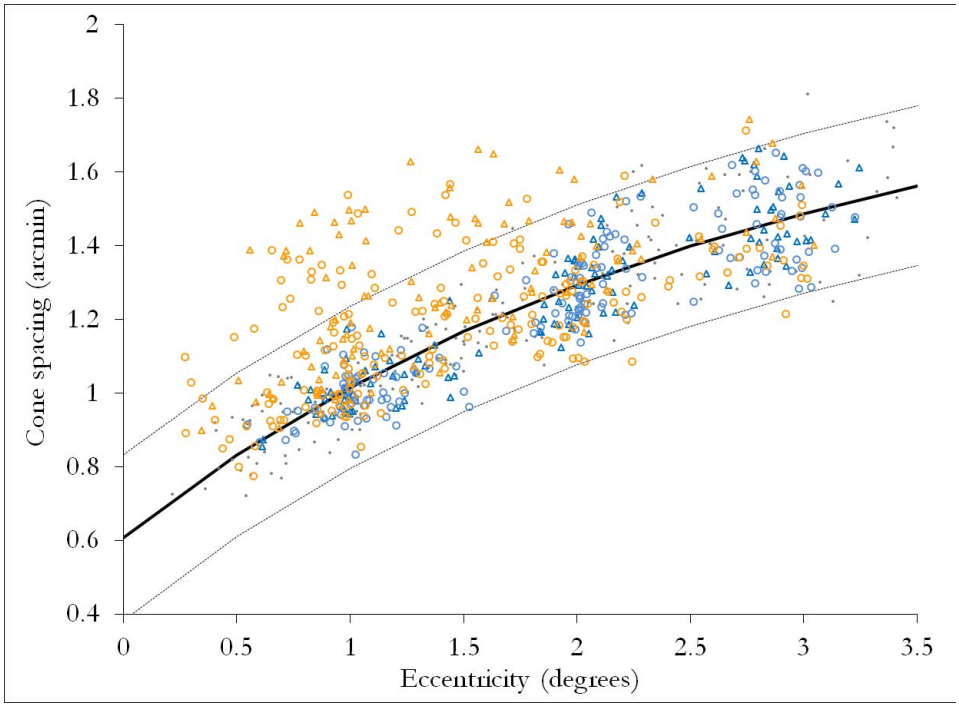

Figure 2. Cone spacing measures correlated with eccentricity as measured by distance from the fovea. The *small black filled circles* represent a normal data set composed of 27 controls.[11] The *dashed curved lines* represent the 95% CI of this normal dataset, and the *solid black line* represents the mean. Normal subjects: *blue*; patients with RD: *orange*; circles: baseline measures; *triangles*: 36-month follow-up measures.

In that study, mean sensitivity values across the visual field spanned from 1–20 dB with a mean value of 13.1 [standard deviation (SD) 4.5] dB in patients, whereas the age-matched normal subject values ranged from 5–20 dB with an average of 14.6 [SD 3.3] dB.[41] The current study used a red filter to deliver red stimuli to optimize cone responses and minimize rod activation because rods are relatively insensitive to longer wavelengths.[42] However, use of the red filter might have contributed to greater variability in threshold responses because the task is more difficult. Another study using the same light-adapted test with red stimuli as in the present study also reported a wide range of sensitivity values spanning across the central visual field.[28]

The current study provides evidence of the correlation between cone spacing Z-scores and macular sensitivity in patients with RD. Although there is a wide range of sensitivity values among the ROIs with Z-scores less than 2, ROIs with Z-scores greater than 2 show reduced sensitivity (Fig. 4C). This provides further evidence that substantial photoreceptor loss is required before it is possible to observe significant decreases in visual function. The current study is aligned with previous studies that showed areas of greater photoreceptor loss with stronger correlations of functional measures, including contrast sensitivity with parafoveal cone density[23] and visual acuity with cone spacing Z-scores within 1 degree of the foveal center.[12,43]

The present study demonstrated significantly increased cone spacing at 36 months compared to baseline in RD patients, measured both in arcminutes and as Z-scores to account for eccentricity. Cone spacing did not change significantly in normal eyes over this 36-month study. Although there was no significant change between baseline and 36 months in IS or OS length, macular sensitivity decreased significantly in patients but not in normal eyes. Due to cone photoreceptor degeneration—particularly in patients studied in the current manuscript with RP and Usher syndrome type 3—a decrease in sensitivity over a period of 36 months is expected and coincides with increased cone spacing or cone loss. Nevertheless, the current study was limited by the number of subjects with sensitivity data at both baseline and 36 months; larger, more prospective studies incorporating fundus-guided microperimetry may demonstrate macular sensitivity to be an even more sensitive measure of disease progression.[28] Some of the variability in sensitivity measures may be due to

Table 4. OS and IS Thickness Correlated With Sensitivity in Normal Eyes but not in RD Patients

OCT Layer Thickness (μm)	Spearman's Correlation ρ Sensitivity (dB)	95% CI	*P* Value	Fig.
IS thickness				
Normal subjects	0.18	0.006 to 0.43	0.047	4A
Patients	0.11	−0.25 to 0.38	0.60	
OS thickness				
Normal subjects	0.36	0.27 to 0.61	<0.001	4B
Patients	0.30	−0.09 to 0.70	0.14	

Table 5. Cone Spacing Correlated with Sensitivity

Sensitivity (dB)	Spearman's Correlation ρ Cone Spacing (Z-scores)	95% CI	*P* Value	Fig.
Normal subjects	−0.22	−0.49 to −0.07	<0.001	4C
Patients	−0.38	−0.67 to −0.08	<0.001	

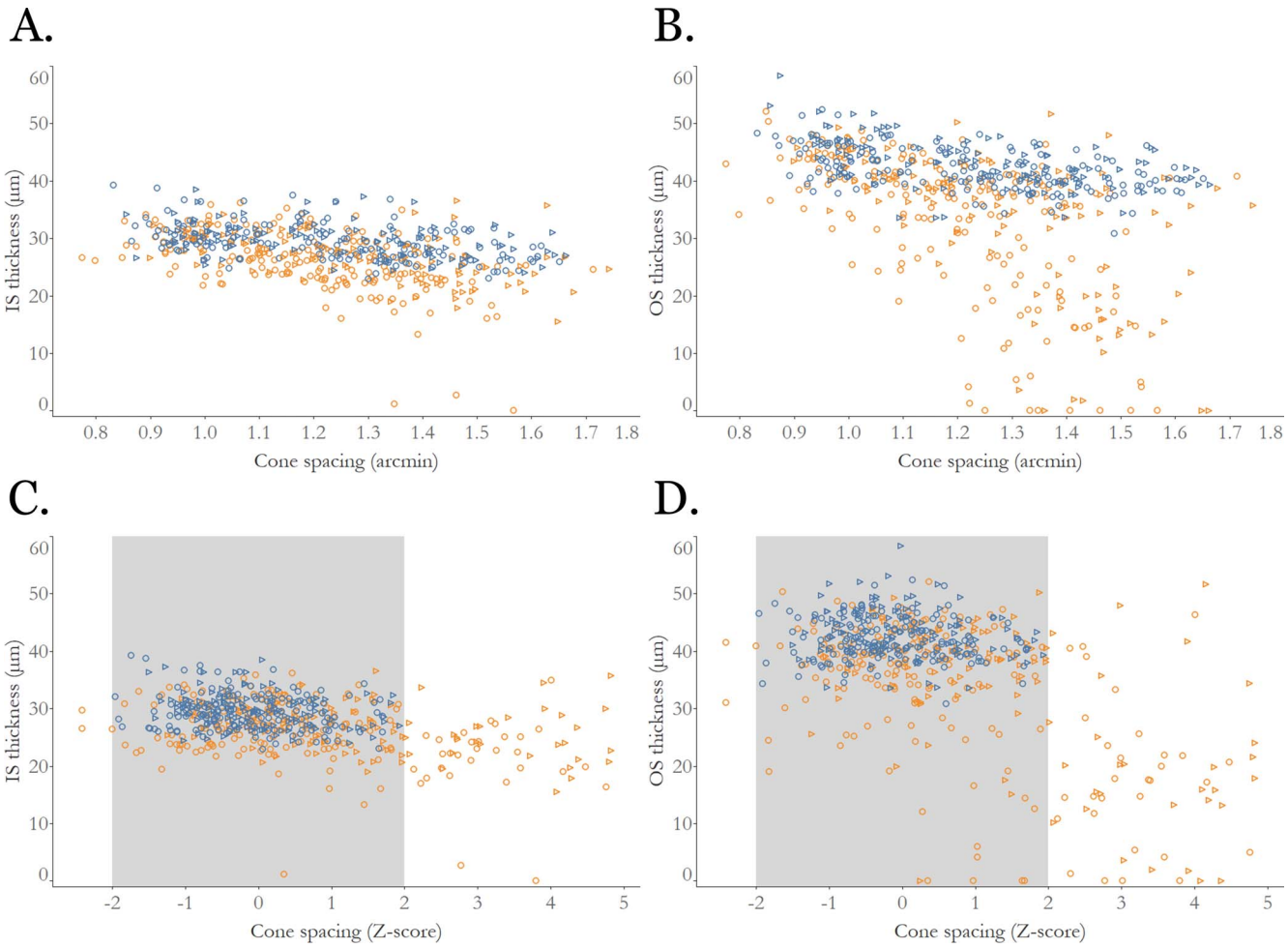

Figure 3. Outer retinal layer thickness correlated with cone spacing measures. (**A**) Inner segment (IS) thickness was significantly correlated with cone spacing in normal subjects and patients. (**B**) Outer segment (OS) thickness was significantly correlated with cone spacing in normal subjects and patients. (**C**) IS thickness was correlated with cone spacing Z-scores in patients but not normal subjects. (**D**) OS thickness was correlated with cone spacing Z-scores in patients but not normal subjects. Normal subjects: *blue*; patients with RD: *orange*; circles: baseline measures; triangles: 36-month follow-up measures. The *gray bands* on graphs C and D indicate the ±2 Z-score limits of normal subjects.

Table 6. Summary of Baseline vs. 36-Month Changes. The *P* Values for the Comparisons Were Considered Significant if Less than 0.05

Outcome Measure	Mean Difference	95% CI	*P* Value
IS thickness (µm)			
Normal subjects	0.78	−0.35 to 1.89	0.18
Patients	0.81	−0.36 to 2.04	0.17
OS thickness (µm)			
Normal subjects	0.66	−0.34 to 2.09	0.22
Patients	−0.66	−1.72 to 0.45	0.22
Cone spacing (arcmin)			
Normal subjects	0.014	−0.009 to 0.030	0.19
Patients	0.1	0.059 to 0.14	<0.001
Cone spacing (Z-scores)			
Normal subjects	0.14	−0.06 to 0.27	0.14
Patients	0.94	0.52 to 1.31	<0.001
Sensitivity (dB)			
Normal subjects	−1.4	−3.78 to 0.93	0.18
Patients	−3.74	−5.56 to −0.81	0.007

discrepancy in background luminance measurements of the liquid crystal display (LCD) used by the fundus-guided microperimetry system in the present study,[44] which has not been observed using other systems that use a super luminescent diode in place of the LCD (MAIA; CenterVue, Inc., Fremont, CA, USA).[45] In addition, fundus-guided microperimetry with commercially available systems does not have resolution commensurate with measures of retinal structure from SD-OCT or AOSLO images. Microperimetry with single cell resolution may improve evaluation of the earliest functional changes in photoreceptor survival. Adaptive Optics Microperimetry (AOMP) enables the precise delivery of visual stimuli to individual cone photoreceptors with a delivery error of 0.89 arcmin,[46] which is less than the cone-to-cone spacing at all eccentricities beyond 1 degree and approximately 5.5 times better at tracking errors of the system used in the present study.[46] Future studies will use AOMP to investigate the relationship between cone spacing Z-scores, IS, and OS thickness and visual sensitivity using this more precise measure of function.

In conclusion, objective measures of photoreceptor structure (such as cross-sectional measures of IS and OS thickness, and cone spacing Z-scores) were significantly correlated with

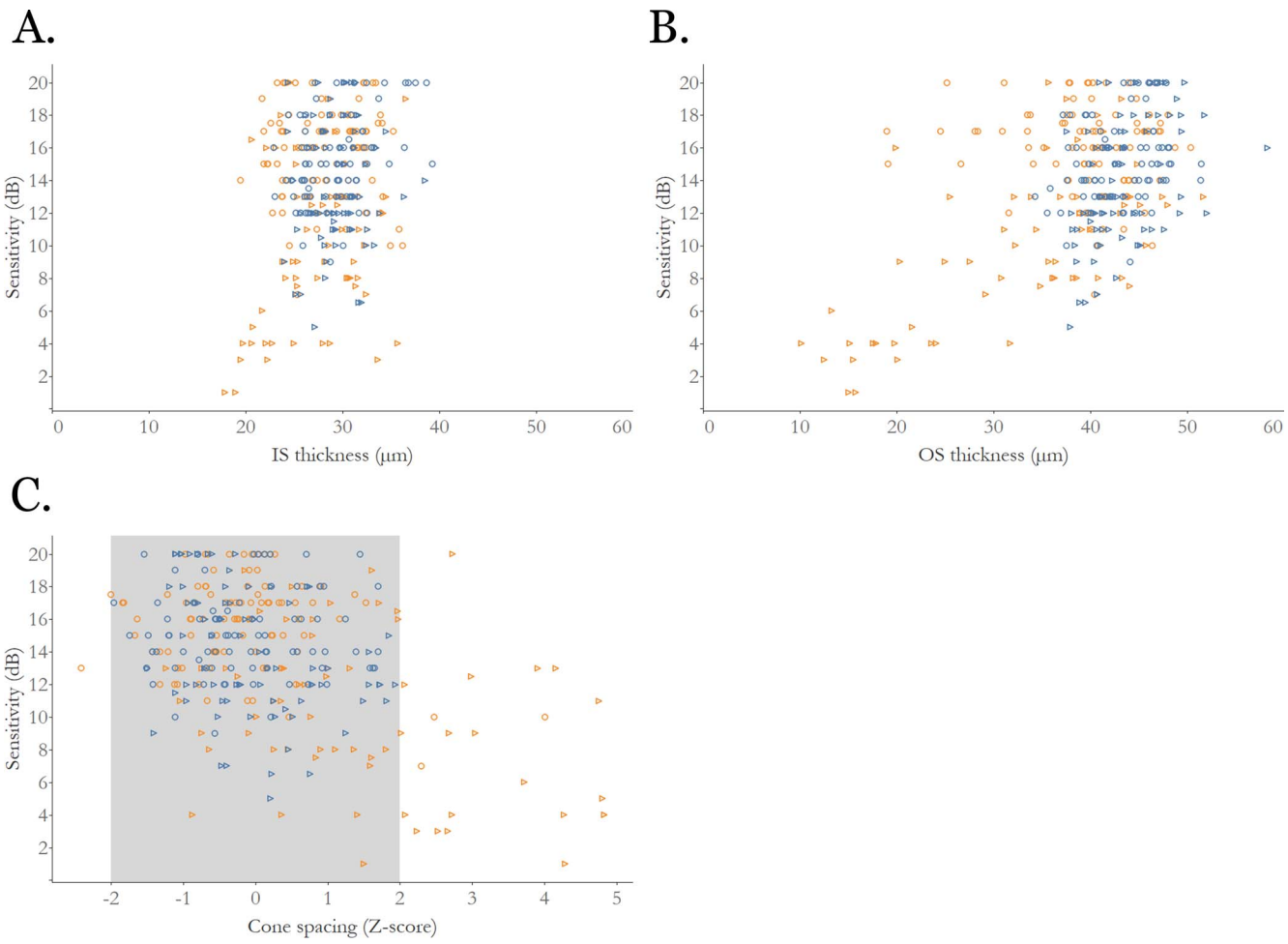

Figure 4. Correlation between outer retinal structure and macular function, measured as retinal sensitivity. (**A**) Retinal sensitivity was correlated with inner segment (IS) thickness in normal eyes but not patients. (**B**) Retinal sensitivity was correlated with outer segment (OS) thickness in normal eyes but not patients. (**C**) Retinal sensitivity was significantly correlated with cone spacing Z-scores in normal and patient eyes. Normal subjects: *blue*; patients with RD: *orange*; circles: baseline measures; *triangles*: 36-month follow-up measures; dB: decibels; the *gray band* in panel C indicates the ±2 Z-score limits of normal subjects.

visual function in patients with retinal degeneration. Cone spacing increased and microperimetry decreased significantly over 36 months in RD patients. These correlations observed suggest that high-resolution images of cone structure can be used to assess patients with RD longitudinally. Furthermore, these correlations between structural measures and visual function may prove to be appropriate outcome measures for clinical trials.

Acknowledgments

Supported by NIH Grant EY023591; NIH Grant EY002162; FDA Grant R01-41001; Foundation Fighting Blindness; Research to Prevent Blindness; Claire Giannini Foundation; L.L. Hillblom Foundation; That Man May See, Inc.; NIH Training Grant 5T32EY007043-37; Minnie Flaura Turner Memorial Fund for Impaired Vision Research Award 2015; National Eye Institute Travel Grant 2017.

Disclosure: **K.G. Foote**, None; **I. De la Huerta**, None; **K. Gustafson**, None; **A. Baldwin**, None; **S. Zayit-Soudry**, None; **N. Rinella**, None; **T.C. Porco**, None; **A. Roorda**, P; **J.L. Duncan**, AGTC (C), California Institute for Regenerative Medicine (C), Foundation Fighting Blindness (C, S), Editas Medicine (C), Ionis Pharmaceuticals (C), Novelion Therapeutics (C), Sparing Vision (C), Spark Therapeutics (C), ProQR Therapeutics (C, R), Allergan (R), Neurotech USA, Inc. (S)

References

1. Hartong DT, Berson EL, Dryja TP. Retinitis pigmentosa. *Lancet*. 2006;368:1795–1809.
2. Robson AG, Michaelides M, Saihan Z, et al. Functional characteristics of patients with retinal dystrophy that manifest abnormal parafoveal annuli of high density fundus autofluorescence; a review and update. *Doc Ophthalmol*. 2008;116:79–89.
3. Birch DG, Locke KG, Felius J, et al. Rates of decline in regions of the visual field defined by frequency-domain optical coherence tomography in patients with RPGR-mediated X-linked retinitis pigmentosa. *Ophthalmology*. 2015;122:833–839.
4. Birch DG, Locke KG, Wen Y, Locke KI, Hoffman DR, Hood DC. Spectral-domain optical coherence tomography measures of outer segment layer progression in patients with X-linked retinitis pigmentosa. *JAMA Ophthalmol*. 2013;131:1143–1150.
5. Hood DC, Cho J, Raza AS, Dale EA, Wang M. Reliability of a computer-aided manual procedure for segmenting optical

coherence tomography scans. *Optom Vis Sci*. 2011;88:113–123.

6. Roorda A, Duncan JL. Adaptive optics ophthalmoscopy. *Annu Rev Vis Sci*. 2015;1:19–50.
7. Roorda A, Romero-Borja F, Donnelly W III, Queener H, Hebert T, Campbell M. Adaptive optics scanning laser ophthalmoscopy. *Opt Express*. 2002;10:405–412.
8. Duncan JL, Zhang Y, Gandhi J, et al. High-resolution imaging with adaptive optics in patients with inherited retinal degeneration. *Invest Ophthalmol Vis Sci*. 2007;48:3283–3291.
9. Sun LW, Johnson RD, Langlo CS, et al. Assessing photoreceptor structure in retinitis pigmentosa and Usher syndrome. *Invest Ophthalmol Vis Sci*. 2016;57:2428–2442.
10. Wolfing JI, Chung M, Carroll J, Roorda A, Williams DR. High-resolution retinal imaging of cone-rod dystrophy. *Ophthalmology*. 2006;113:1014–1019.
11. Chen Y, Ratnam K, Sundquist SM, et al. Cone photoreceptor abnormalities correlate with vision loss in patients with Stargardt disease. *Invest Ophthalmol Vis Sci*. 2011;52:3281–3292.
12. Ratnam K, Carroll J, Porco TC, Duncan JL, Roorda A. Relationship between foveal cone structure and clinical measures of visual function in patients with inherited retinal degenerations. *Invest Ophthalmol Vis Sci*. 2013;54:5836–5847.
13. Talcott KE, Ratnam K, Sundquist SM, et al. Longitudinal study of cone photoreceptors during retinal degeneration and in response to ciliary neurotrophic factor treatment. *Invest Ophthalmol Vis Sci*. 2011;52:2219–2226.
14. Litts KM, Cooper RF, Duncan JL, Carroll J. Photoreceptor-based biomarkers in AOSLO retinal imaging. *Invest Ophthalmol Vis Sci*. 2017;58:BIO255–BIO267.
15. Battu R, Khanna A, Hegde B, Berendschot TT, Grover S, Schouten JS. Correlation of structure and function of the macula in patients with retinitis pigmentosa. *Eye (Lond)*. 2015;29:895–901.
16. Chui TY, Song H, Clark CA, Papay JA, Burns SA, Elsner AE. Cone photoreceptor packing density and the outer nuclear layer thickness in healthy subjects. *Invest Ophthalmol Vis Sci*. 2012;53:3545–3553.
17. Menghini M, Lujan BJ, Zayit-Soudry S, et al. Correlation of outer nuclear layer thickness with cone density values in patients with retinitis pigmentosa and healthy subjects. *Invest Ophthalmol Vis Sci*. 2014;56:372–381.
18. Bruce KS, Harmening WM, Langston BR, Tuten WS, Roorda A, Sincich LC. Normal perceptual sensitivity arising from weakly reflective cone photoreceptors. *Invest Ophthalmol Vis Sci*. 2015;56:4431–4438.
19. Tu JH, Foote KG, Lujan BJ, et al. Dysflective cones: visual function and cone reflectivity in long-term follow-up of acute bilateral foveolitis. *Am J Ophthalmol Case Rep*. 2017;7:14–19.
20. Wang Q, Tuten WS, Lujan BJ, et al. Adaptive optics microperimetry and OCT images show preserved function and recovery of cone visibility in macular telangiectasia type 2 retinal lesions. *Invest Ophthalmol Vis Sci*, 2015;56:778–786.
21. Miller DT, Williams DR, Morris GM, Liang J. Images of cone photoreceptors in the living human eye. *Vision Res*. 1996;36:1067–1079.
22. Milam AH, Li ZY, Fariss RN. Histopathology of the human retina in retinitis pigmentosa. *Prog Retin Eye Res*. 1998;17:175–205.
23. Hirota M, Morimoto T, Kanda H, et al. Relationships between spatial contrast sensitivity and parafoveal cone density in normal subjects and patients with retinal degeneration. *Ophthalmic Surg Lasers Imaging Retina*. 2017;48:106–113.
24. Choi SS, Doble N, Hardy JL, et al. In vivo imaging of the photoreceptor mosaic in retinal dystrophies and correlations with visual function. *Invest Ophthalmol Vis Sci*. 2006;47:2080–2092.
25. Ferris FL III, Kassoff A, Bresnick GH, Bailey I. New visual acuity charts for clinical research. *Am J Ophthalmol*. 1982;94:91–96.
26. Biswas P, Duncan JL, Maranhao B, et al. Genetic analysis of 10 pedigrees with inherited retinal degeneration by exome sequencing and phenotype-genotype association. *Physiol Genomics*. 2017;49:216–229.
27. Ratnam K, Vastinsalo H, Roorda A, Sankila EM, Duncan JL. Cone structure in patients with Usher syndrome type III and mutations in the Clarin 1 gene. *JAMA Ophthalmol*. 2013;131:67–74.
28. Birch DG, Wen Y, Locke K, Hood DC. Rod sensitivity, cone sensitivity, and photoreceptor layer thickness in retinal degenerative diseases. *Invest Ophthalmol Vis Sci*. 2011;52:7141–7147.
29. Hood DC, Lin CE, Lazow MA, Locke KG, Zhang X, Birch DG. Thickness of receptor and post-receptor retinal layers in patients with retinitis pigmentosa measured with frequency-domain optical coherence tomography. *Invest Ophthalmol Vis Sci*. 2009;50:2328–2336.
30. Wen Y, Klein M, Hood DC, Birch DG. Relationships among multifocal electroretinogram amplitude, visual field sensitivity, and SD-OCT receptor layer thicknesses in patients with retinitis pigmentosa. *Invest Ophthalmol Vis Sci*. 2012;53:833–840.
31. Wen Y, Locke KG, Klein M, et al. Phenotypic characterization of 3 families with autosomal dominant retinitis pigmentosa due to mutations in *KLHL7*. *Arch Ophthalmol*. 2011;129:1475–1482.
32. Aizawa S, Mitamura Y, Baba T, Hagiwara A, Ogata K, Yamamoto S. Correlation between visual function and photoreceptor inner/outer segment junction in patients with retinitis pigmentosa. *Eye (London)*. 2009;23:304–308.
33. Rodieck RW. The density recovery profile: a method for the analysis of points in the plane applicable to retinal studies. *Vis Neurosci*. 1991;6:95–111.
34. Makiyama Y, Ooto S, Hangai M, et al. Macular cone abnormalities in retinitis pigmentosa with preserved central vision using adaptive optics scanning laser ophthalmoscopy. *PLoS One*. 2013;8:e79447.
35. Wilk MA, McAllister JT, Cooper RF, et al. Relationship between foveal cone specialization and pit morphology in albinism. *Invest Ophthalmol Vis Sci*. 2014;55:4186–4198.
36. Wilk MA, Wilk BM, Langlo CS, Cooper RF, Carroll J. Evaluating outer segment length as a surrogate measure of peak foveal cone density. *Vision Res*. 2017;130:57–66.
37. Lazow MA, Hood DC, Ramachandran R, et al. Transition zones between healthy and diseased retina in choroideremia (CHM) and Stargardt disease (STGD) as compared to retinitis pigmentosa (RP). *Invest Ophthalmol Vis Sci*. 2011;52:9581–9590.
38. Duncan JL, Talcott KE, Ratnam K, et al. Cone structure in retinal degeneration associated with mutations in the peripherin/RDS gene. *Invest Ophthalmol Vis Sci*. 2011;52:1557–1566.
39. McLaughlin ME, Sandberg MA, Berson EL, Dryja TP. Recessive mutations in the gene encoding the beta-subunit of rod phosphodiesterase in patients with retinitis pigmentosa. *Nat Genet*. 1993;4:130–134.
40. Cai X, Conley SM, Naash MI. RPE65: role in the visual cycle, human retinal disease, and gene therapy. *Ophthalmic Genet*. 2009;30:57–62.

Investigative Ophthalmology & Visual Science

41. Acton JH, Greenberg JP, Greenstein VC, et al. Evaluation of multimodal imaging in carriers of X-linked retinitis pigmentosa. *Exp Eye Res*. 2013;113:41–48.
42. Bowmaker JK, Dartnall HJ. Visual pigments of rods and cones in a human retina. *J Physiol*. 1980;298:501–511.
43. Foote KG, Loumou P, Griffin S, et al. Relationship between foveal cone structure and visual acuity measured with adaptive optics scanning laser ophthalmoscopy in retinal degeneration. *Invest Ophthalmol Vis Sci*. 2018;59:3385–3393.
44. Springer C, Bultmann S, Volcker HE, Rohrschneider K. Fundus perimetry with the Micro Perimeter 1 in normal individuals: comparison with conventional threshold perimetry. *Ophthalmology*. 2005;112:848–854.
45. Wong EN, Mackey DA, Morgan WH, Chen FK. Inter-device comparison of retinal sensitivity measurements: the CenterVue MAIA and the Nidek MP-1. *Clin Exp Ophthalmol*. 2016;44:15–23.
46. Tuten WS, Tiruveedhula P, Roorda A. Adaptive optics scanning laser ophthalmoscope-based microperimetry. *Optom Vis Sci*. 2012;89:563–574.

Investigative Ophthalmology & Visual Science